

Dendrimicelles with pH-controlled aggregation number of core-dendrimers and stability

Junyou Wang,^{a,b} Lei Liu,^a Ilja K. Voets,^c Martien A. Cohen Stuart,^a Aldrik H. Velders^{b*}

a: State-Key Laboratory of Chemical Engineering and Shanghai Key Laboratory of Multiphase Materials Chemical Engineering, East China University of Science and Technology, Shanghai 200237, People's Republic of China

b: Laboratory of BioNanoTechnology, Wageningen University, Dreijenplein 6, 6703 HB Wageningen, The Netherlands

c: Laboratory of Macromolecular and Organic Chemistry, Department of Chemistry and Chemical Engineering, and Institute for Complex Molecular Systems, Eindhoven University of Technology, P.O. Box 513, 5600 MB Eindhoven, The Netherlands

*To whom correspondence should be addressed:

E-mail: aldrik.velders@wur.nl

This file includes:

1. Experimental section; (Table S1)
2. Light scattering titration curve of G3-C3Ms at pH 8, 9, 11; (Figure S1)
3. Angular dependence and zeta potential of G3-C3Ms at different pH (Figure S2)
4. SAXS profiles and data fitting of G3-C3Ms at different pH; (Figure S3 & Table S2)
5. Determination of micellar mass and aggregation number (Figure S4 & Table S3)
6. Determination of CMC (Figure 5 & Table S4)
7. Salt titration and determination of critical salt concentration; (Figure S6 & Table S5)
8. References.

1. Experimental section

Materials

The carboxylate terminated PAMAM dendrimer (G3) was purchased from Sigma Aldrich. The original solvent methanol was evaporated carefully under N₂ and the obtained compound was dissolved in nanopure water. The diblock copolymer, poly(N-methyl-2-vinyl-pyridinium iodide)-*b*-poly(ethylene oxide) (P2MVP₁₂₈-*b*-PEO₄₇₇), was obtained by quaternization of poly(2-vinylpyridine)-*b*-poly(ethylene oxide) (P2MVP₁₂₈-*b*-PEO₄₇₇) (Polymer Source, M_w/M_n= 1.10, M_n= 34.5 k) following a procedure described elsewhere.¹ The degree of quaternization is about 87% as determined by titration with poly(acrylic acid) (PAA, Polymer Source, M_w/M_n= 1.16, M_n= 2.2 k) in water at pH 7. The micelles were prepared by mixing solutions of P2MVP₁₂₈-*b*-PEO₄₇₇ and PAMAM dendrimer in water with 20 mM NaCl, the pH is adjusted with either 0.1 M NaOH or 0.1 M HCl.

Methods

Dynamic and static light scattering

Light scattering at an angle of 90° was performed with an ALV light scattering-apparatus, equipped with a 300 mW cobalt samba DPSS laser operating at a wavelength of 532.0 nm. All measurements were performed at room temperature. Titrations were carried out using a Schott-Geräte computer-controlled titration setup to control sequential addition of titrant and cell stirring. After every dosage, the laser light-scattering intensity (I) and the correlation function were recorded. The hydrodynamic radius and the scattered intensity were studied as a function of the amount of positive charges added in the solution.

The light scattering intensity is expressed as the excess Rayleigh ratio R_θ obtained as

$$R_\theta = \frac{I_{sample} - I_{solvent}}{I_{toluene}} \times R_{toluene} \times \frac{n_{solvent}^2}{n_{toluene}^2} \quad (1)$$

where I_{sample} is the scattering intensity of the micellar solution and $I_{solvent}$ is the intensity of the solvent. $I_{toluene}$ is the scattering intensity of toluene, $R_{toluene}$ is the known Rayleigh ratio of toluene ($2.1 \cdot 10^{-2} \text{ m}^{-1}$) and n is the refractive of solvent (1.333) and toluene (1.497). The total polymer concentration is the sum of the concentrations of dendrimer and diblock copolymer contributing to micelle formation. The micellar size and size distribution is obtained from the CONTIN method.^{2,3} The data were analyzed with the AfterALV program (AfterALV 1.0d, Dullware), which provides $\Gamma_i W_i$ as default output for each size fraction. Here, the intensity weighted contribution W_i is multiplied by Γ , as described by Petr Stepanek for the “equal-area representation”.⁴ To facilitate a comparison between different samples, the absolute $\Gamma_i W_i$ was normalized with the highest value of $\Gamma_i W_i$ for each sample.

The Rayleigh ratio can be linked to the concentration and mass of the scattering objects:

$$\frac{K_R C}{R_\theta} = \frac{I}{M} \times \frac{I}{P(qR)} \times \frac{I}{S(q)} \quad (2)$$

where C is the weight concentration of micelles, M is their molecular mass, and R is the radius of the object that contribute to scatter light. $P(qR)$ and $S(q)$ are the form factor and the structure factor, respectively. K_R is an optical constant defined as:

$$K_R = \frac{4\pi^2 n^2}{N_{Av} \lambda_0^4} \left(\frac{dn}{dc} \right)^2 \quad (3)$$

where n is the refractive index of solvent, N_{Av} is Avogadro’s number, λ_0 is the wavelength of the incoming beam (532.0 nm), and dn/dc is the refractive index

increment of the micelles. dn/dc of the micelles at different pH is estimated by a weighted average of the refractive index increment of the polymeric components (2.02×10^{-4} , $1.95 \times 10^{-4} \text{ m}^3/\text{kg}$ for G3-PAMAM and P2MVP₁₂₈-*b*-PEO₄₇₇)⁵ and the results are shown in Table S1.

pH	7	8	9	10	11
$dn/dc \cdot 10^4$ $\text{m}^3 \text{ kg}^{-1}$	1.98	1.97	1.97	1.97	1.97

Table S1 dn/dc of G3-C3Ms formed at different pH.

In our experiments, the scattering vector $q = (4\pi n/\lambda_0)\sin(\theta/2)$ is approximately 0.023 nm^{-1} ($\theta = 90^\circ$), so that qR is small for the micelles. We therefore assume that $P(qR)=1$.

At low concentrations, the structure factor can be approximated as

$$\frac{I}{S(q)} = 1 + 2B_2 \frac{C}{M} \quad (4)$$

where B_2 is the second virial coefficient. Substitution into equation 4, we get

$$\frac{K_R C}{R_\theta} = \frac{I}{M} + 2B_2 \frac{C}{M^2} \quad (5)$$

By plotting $K_R C/R_\theta$ versus C , we can obtain the molar mass M from the intercept. In our study, M corresponds to the molar mass of micelles, $M_{micelle}$, from which we can calculate the aggregation number of the micelles, see Figure S2.

Small angle X-ray scattering

Small angle X-ray scattering experiments were performed on a Ganesha lab instrument equipped with a GeniX-Cu ultra low divergence source producing X-rays with a

wavelength of 1.54 Å and a flux of 1×10^8 ph/s. Scattering patterns were collected on a Pilatus 300K silicon pixel detector (487 x 619 pixels of 172 x 172 μm) at two sample-to-detector distances corresponding to 730 and at 1530 mm covering a q range of $6.7 \times 10^{-2} < q < 4.45 \text{ nm}^{-1}$. The position of the beam center and the q range were calibrated using the diffraction peaks of silver behenate. The liquid samples were contained in 2 mm quartz capillaries sealed and fixed in a stainless steel holder kept at room temperature. The sample concentration was fixed at a dendrimer charge concentration of 2mM in all cases. The scattering data were corrected for background contributions (such as scattering from the buffer solution), detector response and primary beam intensity fluctuations. The SAXS data were treated and analyzed using the software packages SAXSGUI and SASVIEW.

2. LS titration curve of G3-C3Ms at pH 8, 9, 11

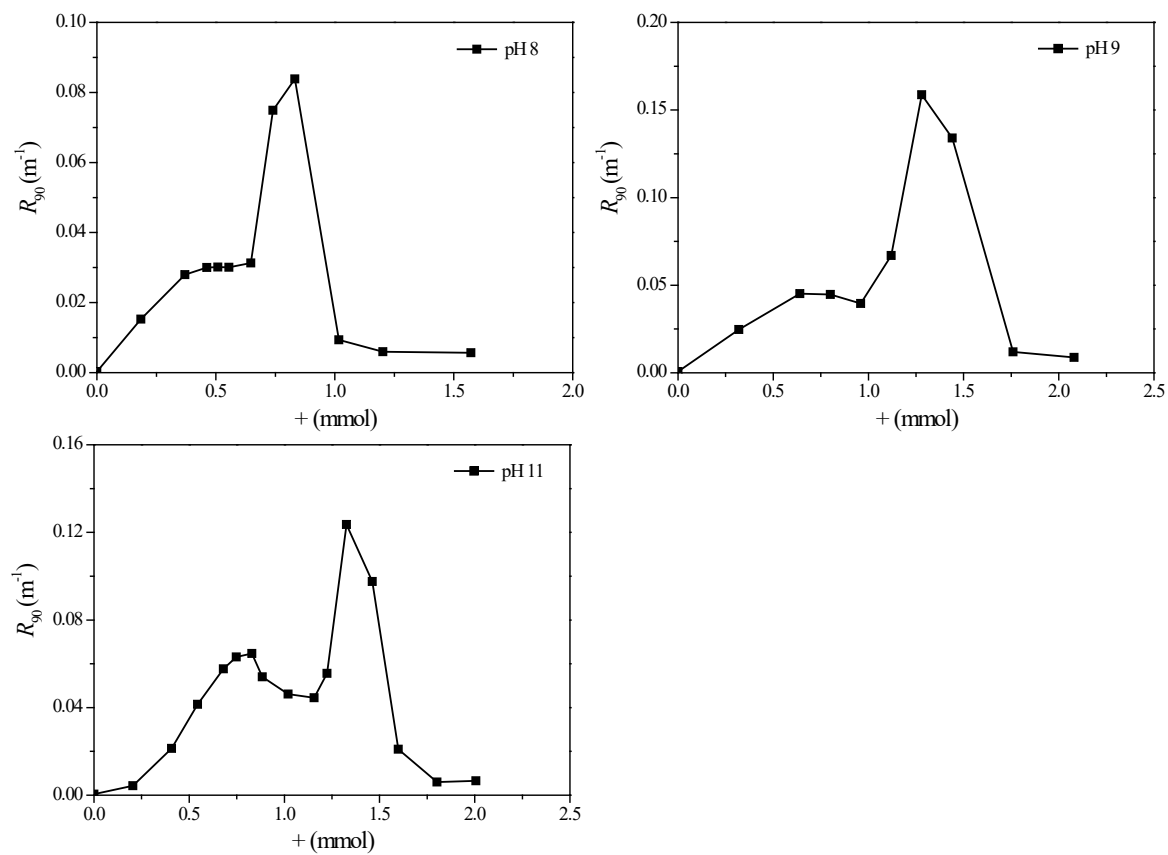


Figure S1 light scattering titration curve of G3-C3Ms at pH 8, 9, 11. The intensity is expressed by the excess Rayleigh ratio R_{θ} , (experiment part, equation 1) and plotted as a function of amount of positive charges added in the dendrimer solution.

3. Angular dependence and zeta potential measurements

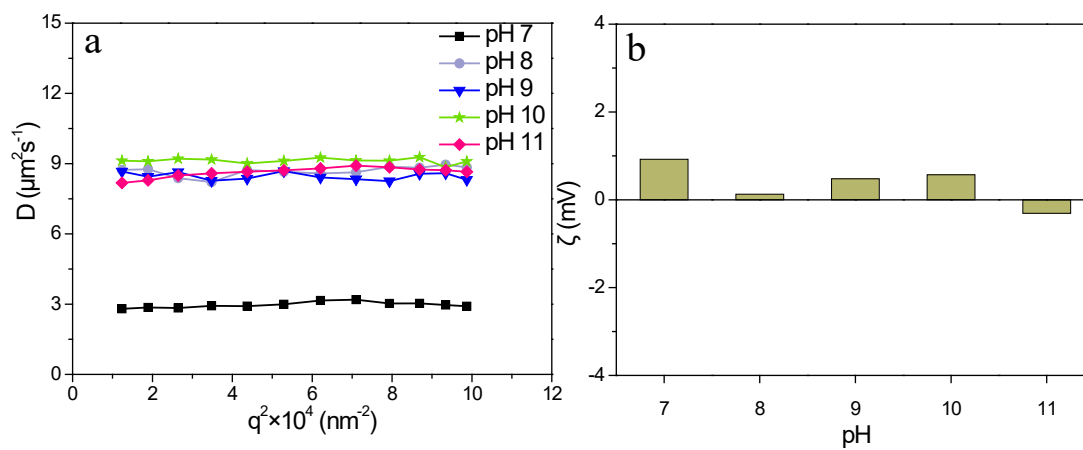


Figure S2 Angular dependence of the self-diffusion coefficient and ζ -potential of G3-C3Ms at different pH. All micelles were prepared at PMC charge ratio.

4. SAXS profiles and data fitting

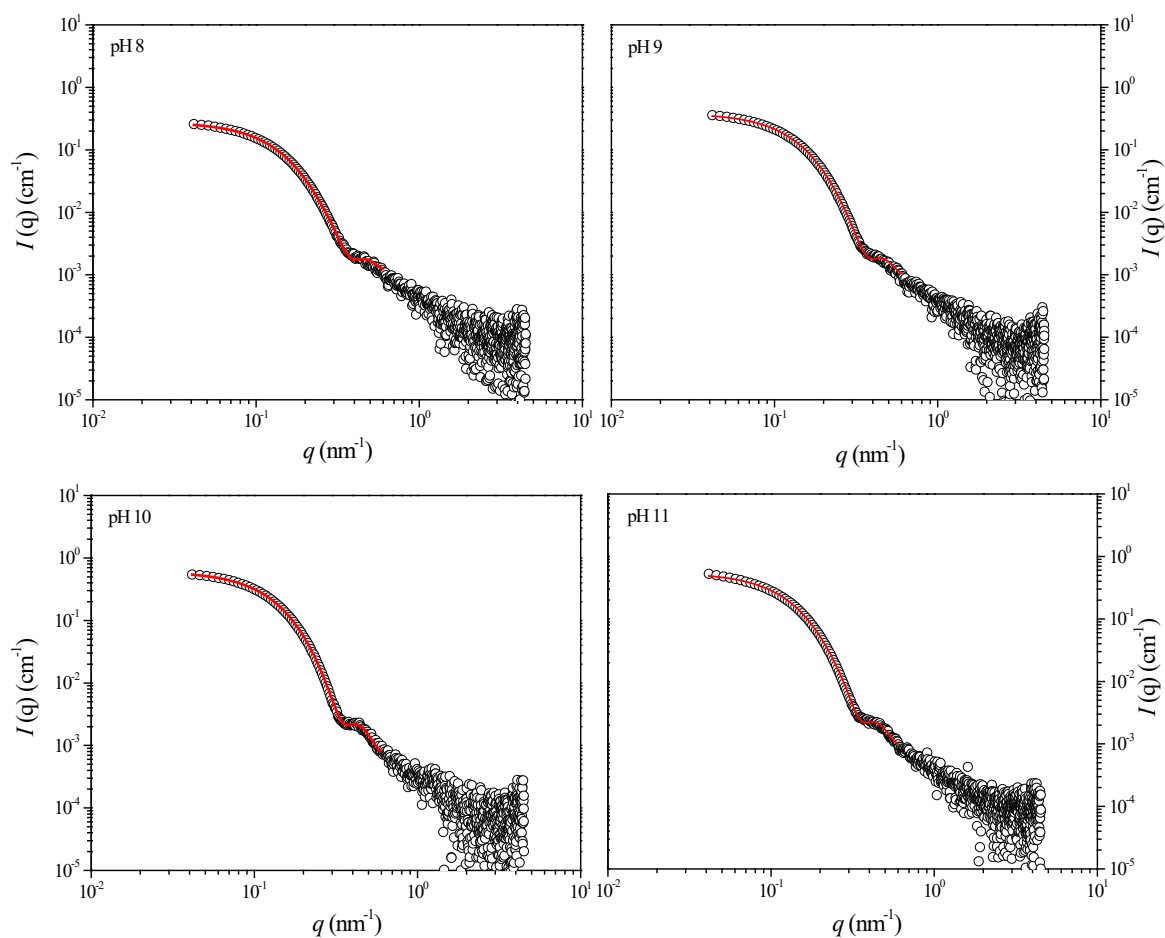


Figure S3 SAXS profiles of G3-C3Ms at different pH. The open circles shows the experimental data and the solid red line corresponds to the fits with a form factor for polydisperse (Gaussian distribution) core-shell spheres. The scattering length density of solvent, micellar core, shell are 9.37, 11.11, 9.45 (10^{10} cm^{-2}), respectively, and the dispersity ratio is $\sim 16\%$.

pH	8	9	10	11
R_h (nm)	24.1	24.6	24.7	24.7
R_{core} (nm)	11.2	11.4	12.2	11.9
H_{shell} (nm)	12.6	12.3	12.7	12.7

Table S2 Obtained hydrodynamic radius (R_h), core radius (R_{core}) and shell thickness (H_{shell}) of G3-C3Ms at different pH.

5. Determination of the micellar mass and aggregation number

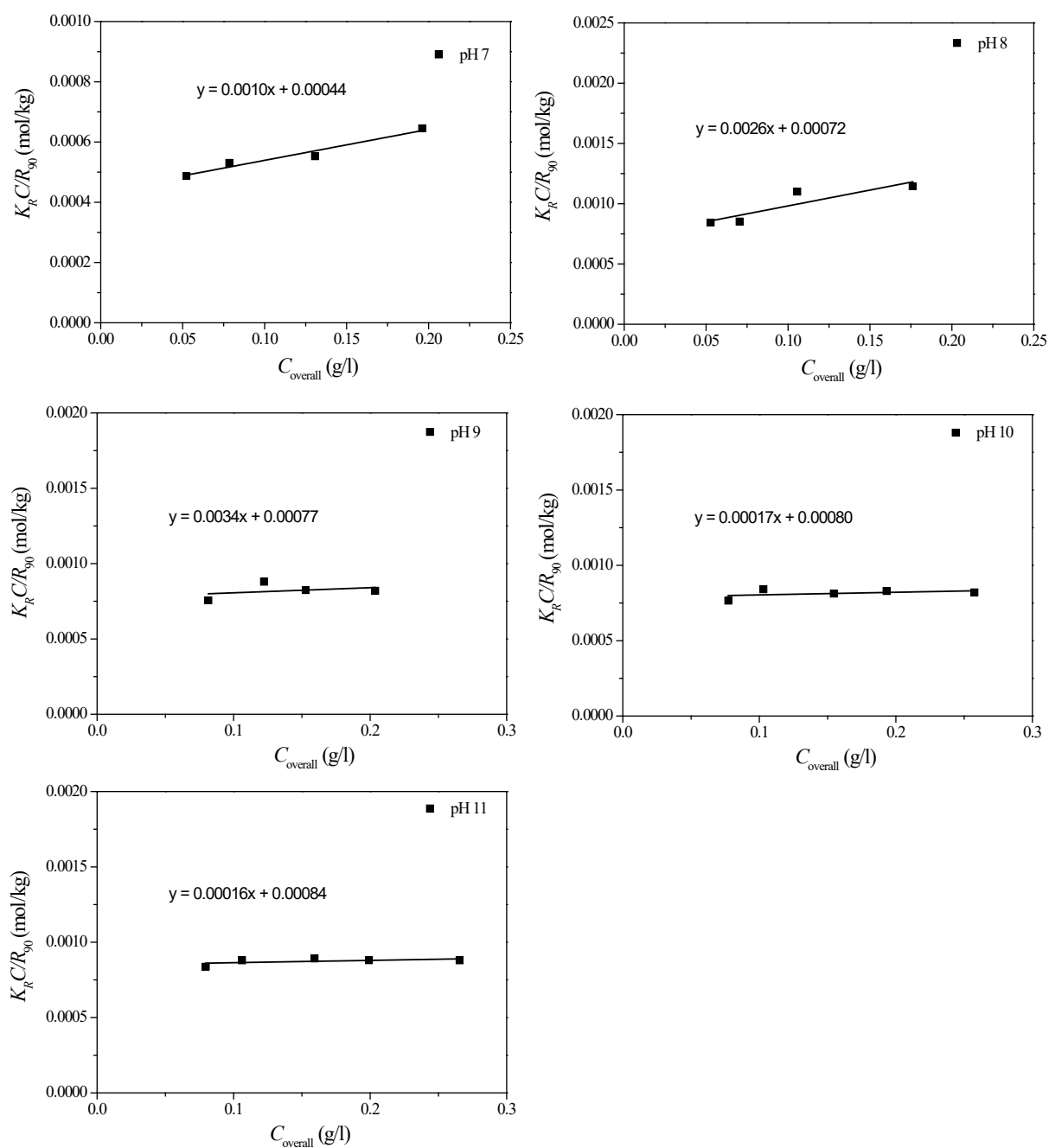


Figure S4 $K_R C/R_{90}$ is plotted as a function of C_{overall} . Here C_{overall} is the total concentration of P2MVP_{128-b}-PEO₄₇₇ polymer and dendrimer subtracted by CMC, and CMC is obtained from Table S4.

The final micelle are neutralized structures. Based on the consumed amount of positive charges, which is the amount at PMC in light scattering titration curve (Figure 1a, S1),

we calculate the actual charge numbers of dendrimer at different pH. (Table S2) Together with the micellar mass, M_{micelle} obtained from the intercept of K_{RC}/R_{90} vs C_{overall} plot, we can calculate the aggregation number of dendrimer and diblock copolymer. For example, at pH 10, we get micellar mass:

$$M_{\text{micelle}} = 1/0.00080 = 1250 \text{ kg/mol} = 1250 \times 10^3 \text{ g/mol}$$

The charge numbers, Z and molecular weights of dendrimer and polymer are

$$\begin{aligned} Z_{\text{pH } 10} &= 32, & M_{\text{G3}} &= 6256.6, \text{ (g/mol)} \\ Z_{\text{polymer}} &= 128 \times 0.87 = 111, & M_{\text{polymer}} &= 50313 \text{ (g/mol)} \end{aligned}$$

At PMC point: $N_{\text{polymer}} \times 111 = N_{\text{G3}} \times 32$ (6)

Moreover, the molar masses of dendrimer, polymer and micelle are recorded as follows:

$$N_{\text{G3}} \times 6256.6 + N_{\text{polymer}} \times 50313 = 1250 \times 10^3$$
 (7)

Solving equation 6 and 7, we find that $N_{\text{G3}} = 17.3$ and $N_{\text{polymer}} = 60.2$. Following the same strategy, we calculated the aggregation number of G3 (32 –COONa groups) based C3Ms at other pH, see the table below:

pH	7	8	9	10	11
Dissociation degree α	56%	78%	87%	100%	100%
Charge number per dendrimer	18	25	28	32	32
N_{G3}	157.6	82.2	68.5	60.2	56.8
N_{polymer}	25.6	17.8	17.3	17.3	16.4

Table S3 Dissociation degree of the –COONa and surface charge of dendrimer, micellar mass and aggregations numbers of G3-C3Ms at different pH. The relative error in the calculation is $\sim 15\%$, estimated by summation of the errors from determining the PMC (8%), CMC (2%) and polymer concentration (5%).

6. Determination of the CMC of G3-C3Ms

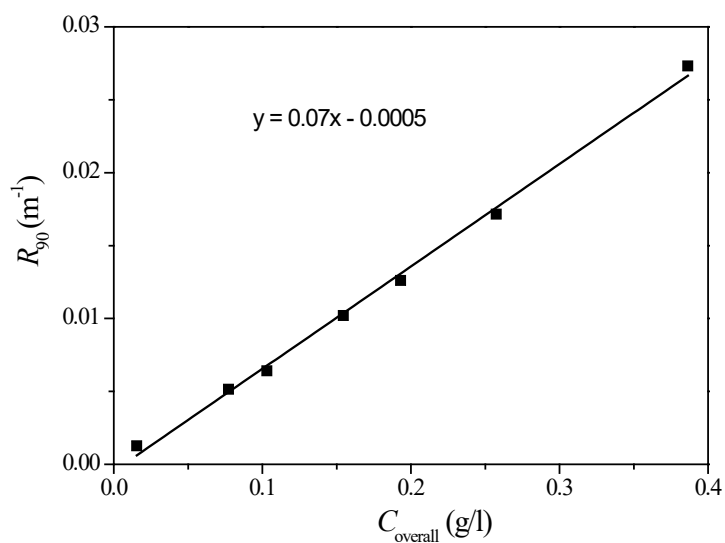


Figure S5 Intensity decay of G3-C3Ms at pH 10 upon diluting with pH 10 water. The filled squares are the experimental data and the solid line is the fitting curve.

The intensity is represented as Rayleigh ratio R_{θ} , which is subtracted with the intensity from buffer solution and corrected by the intensity of toluene as a reference, see experimental section, method, equation 1. The CMC is determined by extrapolating the decay line to zero intensity, and calculated from the fitting formula. The CMCs of the micelles formed at other pHs are obtained following same way, and the numbers are included in the table below:

pH	7	8	9	10	11
CMC g/l	0.03	0.02	0.04	0.01	0.01

Table S4 CMC of G3-C3Ms formed at different pH.

7. Determination of critical salt concentration

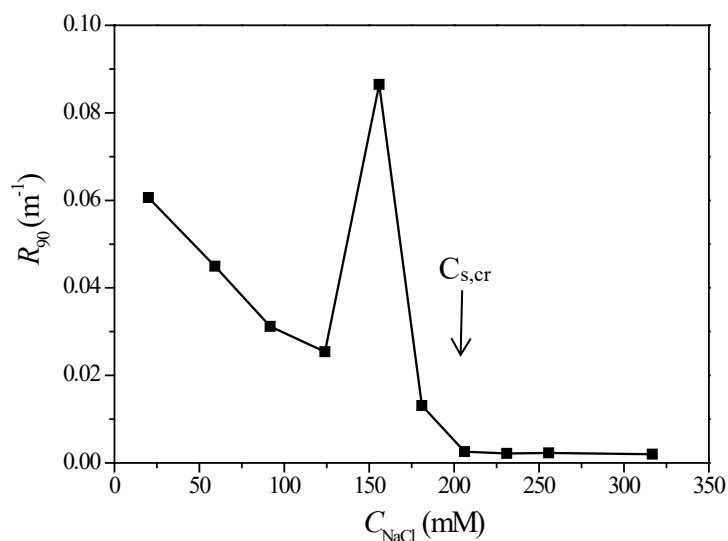


Figure S6 variation of the LS intensity upon titration NaCl in the micellar solution at pH 10. The arrow shows the position of the critical salt concentration. Salt titration of G3-C3Ms at other pHs give the similar curves and the obtained critical salt concentration are summarized in Table S5.

pH	7	8	9	10	11
$C_{s,cr}$ mM	55	75	115	194	191

Table S5 Critical salt concentration of G3-C3Ms at different pH.

The jump of the intensity in the titration curve may be due to the morphology transition from sphere to elongated structures. We find the similar changes in previous studies with both linear polyelectrolytes and dendrimer based C3Ms.^{5,6}

8. Reference:

1. M. Biesalski, D. Johannsmann and J. Ruhe, *J. Chem. Phys.*, 2004, **120**, 8807-8814.
2. S. W. Provencher, *Comput. Phys. Commun.*, 1982, **27**, 213-227.
3. S. W. Provencher, *Comput. Phys. Commun.*, 1982, **27**, 229-242.
4. P. Stepanek, *In Dynamic Light Scattering: the method and some applications; Brown, D., Ed.; Clarendon Press: Oxford, U. K., 1993, Chapter 4*, 177.
5. H. M. van der Kooij, E. Spruijt, I. K. Voets, R. Fokkink, M. A. Cohen Stuart and J. van der Gucht, *Langmuir*, 2012, **28**, 14180-14191.
6. J. Y. Wang, I. K. Voets, R. Fokkink, J. van der Gucht and A. H. Velders, *Soft Matter*, 2014, **10**, 7337-7345.